18th Australasian Fluid Mechanics Conference
Launceston, Australia
3-7 December 2012

Numerical Investigation of Diaphragm Mass and Viscous Effects on Pulse Starting of Axisymmetric Scramjet Inlets

H. Ogawa[1], S. Mölder[2] and R. R. Boyce[3]

[1]Centre for Hypersonics
University of Queensland, Brisbane, QLD 4072, Australia

[2]McGill University
Montreal, Quebec H3A 2K6, Canada

Abstract

Scramjets are a promising hypersonic airbreathing technology for economical access-to-space and atmospheric transport. Reliable scramjet inlet starting is of crucial importance for successful scramjet operation. It is shown that unsteady flow, resulting from the rupture of a diaphragm, can result in a steady started inlet flow. Time-accurate computations illustrate flow and wave motion during the unsteady starting process. The effects of viscosity and diaphragm mass on the inlet flowfields are investigated by time-accurate computational simulations.

Introduction

Hypersonic airbreathing propulsion offers great potential for reliable and economical access-to-space as well as atmospheric flight. In particular, scramjets (Supersonic Combustion Ramjets) are a promising technology that can enable efficient and flexible transport systems by removing the need to carry oxidisers and other propulsion limitations that are necessary for conventional rocket engines. The SCRAMSPACE program is now underway as an international collaboration led by The University of Queensland [1], where axisymmetric scramjet configurations featuring various innovative concepts such as fuel injection on the inlet surface and shock-induced combustion by radical-farming are being investigated in both ground and flight tests.

High internal compression axisymmetric inlets are inherently difficult to start spontaneously during flight. The flow inside the scramjet engine must be supersonic throughout in normal operation in the 'started' case. However, high contraction inlets can also operate in an 'unstarted' mode, where the flow is restricted to the extent that it becomes subsonic throughout behind an external bow shock. This results in a dramatic reduction in inlet mass capture and engine thrust. This "inlet starting" issue is intrinsic to internal compression axisymmetric geometries because the structure does not allow surplus mass flow to spill overboard. Unstarted flow is predominantly experienced by high-compression inlets in in-flight operation, thus requiring auxiliary methods to start the inlet, where supersonic started flow can be sustained once it is established. A variety of methods for starting high-compression inlets have been developed, due to the importance of this issue. Variable geometries have been found to be effective in starting the inlet in a quasi-steady manner by regulating the mass flow entry [5,8]. Instantaneous rupture of temporary diaphragms has also demonstrated the capability of starting the inlet because the induced unsteady flow phenomena can effectively circumvent the Kantrowitz criterion, which prescribes the inlet startability under inviscid quasi-steady assumptions [5,7]. The present paper focuses on the latter approach, in particular, the rupture of normal (flat) diaphragms placed at the entry of axisymmetric intakes.

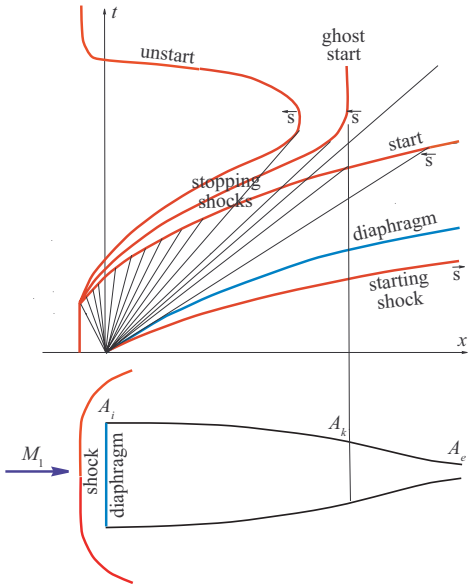

Figure 1. Schematic diagram of inlet starting with normal diaphragm rupture (bottom) and motion of starting and stopping shocks after diaphragm rupture (top).

The lower portion of Figure 1 shows a contracting air intake that is closed off at its entry by a flat *diaphragm*. The intake's axis is aligned with a supersonic flow from the left. There is initially no flow inside the intake, where the pressure is low, and the outside flow is that of a bluff body with a bow shock at the front. The entry and exit areas are denoted by A_i and A_e and the Kantrowitz area by A_k, as obtained from the normal shock theory and area-Mach number relation. The time-history of the diaphragm, after instantaneous rupture/release of the diaphragm, and resulting wave motion, are shown in the upper (x, t)-portion of the figure. On release, the diaphragm moves and accelerates to the right, preceded by the right-facing *starting shock*. The starting shock accelerates to the right and moves out through the exit. From the time/place of rupture an expansion fan propagates to the left into the near-stagnant flow behind the bow shock. On overtaking the bow shock, it causes the bow-shock to accelerate to the right and move into the intake. The bow-shock is left-facing and hence continues to have the capability to move to the left to unstart the intake flow – hence it is re-labelled as the *stopping shock*.

Depending on the degree of intake contraction, the freestream Mach number and the diaphragm pressure ratio, the stopping shock can have one of three characteristic histories. For high contraction and high post-diaphragm pressure the stopping shock reverses its downstream motion, moves upstream to take up a position in front of the intake with steady, subsonic flow inside

the intake. The intake is then *unstarted.* For moderate contraction and low diaphragm pressure the stopping shock continues its motion to the right, out through the exit. Flow to the left of the stopping shock is then steady and supersonic and the intake is *started.* Critical motion of the stopping shock occurs at the Kantrowitz position x_k, where the local cross sectional area is A_k. If the stopping shock reaches a position downstream of x_k it will continue moving downstream and the intake will start. If the stopping shock stops upstream of x_k, it will reverse its motion and the intake will not start. It is possible for the stopping shock to move very slowly or indeed to stop, in a neutrally stable position, at the Kantrowitz position. In this situation there is no bow-wave but the exit flow is subsonic. A *ghost-start* occurs. The above is a simplified one-dimensional explanation of wave motion resulting from diaphragm rupture and intake starting/non-starting. In reality flow is complicated by viscous and 3D flow effects.

A numerical study is undertaken to investigate the mechanism which dictates inlet startability of a pulse-starting method based on unsteady flow effects. Numerical results are compared with analysis. The effects of diaphragm mass and viscosity are examined, with particular focus on the motion of the starting and stopping shocks.

Approaches

Flow Conditions and Configurations

The present study focuses on the internal flowfield in the axisymmetric scramjet intake. The captured airflow is a uniform freestream at Mach 8 with a static pressure and temperature of 1197 Pa and 226.5 K, respectively, wtih scramjet operation at an altitude of 30 km on a constant dynamic pressure trajectory of 53.6 kPa. The Reynolds number based on the nominal inlet exit radius of 0.1 m is 1.79×10^6. The contour for the full Busemann intake is obtained analytically from the Taylor-Maccoll equation, the contraction ratio being 11.2.

Computational Fluid Dynamics

The inlet flowfields are computed by utilising a commercial high-fidelity code CFD++. An advanced wall-function technique is used for near-wall treatment and turbulence is modelled by the two-equation SST k-ω RANS model. The airflow is treated as calorically perfect gas and the inlet surface is assumed to be adiabatic. The patched boundary condition is employed for the diaphragm, which is initially assumed to be an adiabatic wall and switched to a flow-through condition upon rupture. In the case of simulations for a diaphragm with mass, the diaphragm is assumed to have a finite thickness of 5 mm, filled with perfect gas heavier than air. A commercial grid generator Pointwise is utilised to generate two-dimensional structured computational meshes comprising 70,400 cells, where the diaphragm is represented by a rectangular mesh comprising 2×100 cells. The minimum cell thickness on the wall is 10^{-5} m for the viscous mesh. This mesh resolution is selected, based on the mesh dependency study conducted in a preceding study [5].

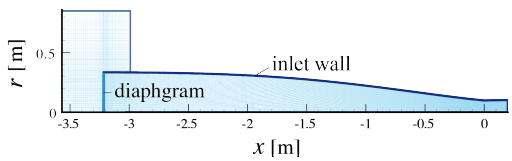

Figure 2. Computational mesh for inlet starting simulation with normal diaphragm rupture (the above is the mesh used for viscous computation employing a diaphragm with finite thickness).

Results

Starting and Stopping Shocks

A time-accurate simulation has been performed for an inviscid flowfield in a full Busemann intake after instantaneous rupture of a normal diaphragm with an initial plenum pressure of $p_i = 0.01p_\infty$. Figure 3 shows the starting and stopping shocks in the early flow phase, 0.8 ms after diaphragm rupture. Both shocks are moving to the right, as shown in the following figure (Figure 4).

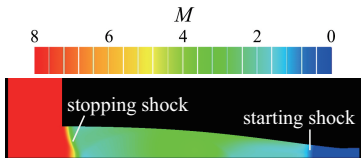

Figure 3. Stopping and starting shocks travelling downstream in the full Busemann inlet (0.8 ms after normal diaphragm rupture).

Snapshots of representative time frames are displayed in Figure 4, where the focal point of the Busemann intake is denoted by a black circle. Plotted in Figure 5 is the motion of the stopping shock obtained from CFD, compared with the prediction from the CCW (Chester-Chisnell-Whitham) relation, which describes the motion of a shock wave travelling into a uniform quiescent gas through a duct with variable cross-sectional area [2]. It can be seen that after the starting shock passes the inlet exit (throat) at about $t = 1$ ms, the stopping shock keeps travelling downstream and moves very slowly near the Kantrowitz position at $t = 3.2$ - 4 ms. The inlet is started at $t = 5$ ms, with a fully supersonic flowfield established.

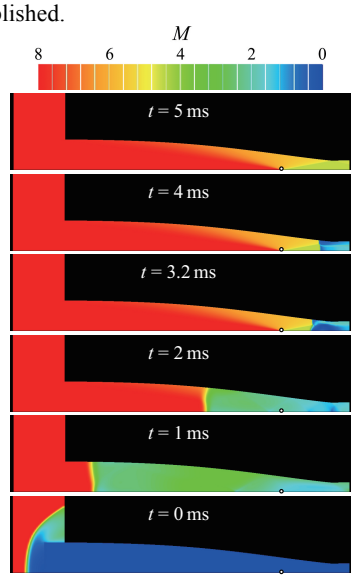

Figure 4. Mach number distribution for an inviscid flowfield after diaphragm rupture calculated by CFD for an initial plenum pressure of $p_i = 0.01p_\infty$ (leading to started inlet).

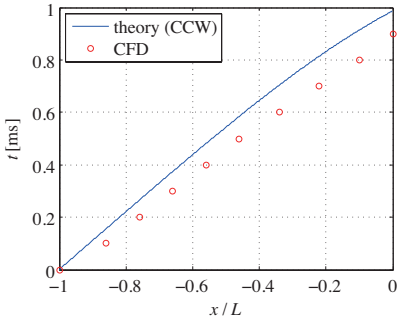

Figure 5. Trajectory of the starting shock travelling downstream in the full Busemann inlet predicted from the CCW theory in comparison with CFD ($p_i = 0.01p_\infty$, L is the total length of the full Busemann inlet).

Figure 6 shows the snapshots of the transient flowfield for diaphragm rupture with a slightly higher initial plenum pressure of $p_i = 0.02p_\infty$. The flowfield is similar until $t = 3.2$ ms, when the stopping shock approaches the Kantrowitz position x_k, but cannot pass the point and reverses its direction, eventually leading to an unstarted inlet at about $t = 10$ ms (not presented).

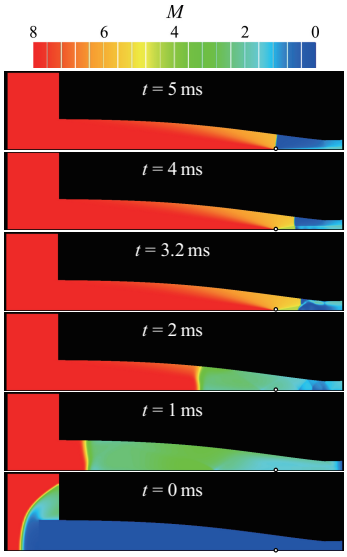

Figure 6. Mach number distribution for an inviscid flowfield after diaphragm rupture calculated by CFD for an initial plenum pressure of $p_i = 0.02p_\infty$ (leading to unstarted inlet).

An analytical approach based on the shock-tube equation [2] is applied to evaluate the influence of the initial plenum pressure ratio p_i / p_∞ on the behaviour of the starting and stopping shocks. This approach accounts for the effect of the overtaking of the stopping shock by an expansion fan [3]. The results are plotted in Figure 7, where M_{98} is the starting shock number, M_8 the Mach number of the gas behind the starting shock, M_{12} the stopping shock number, M_2 the Mach number of the gas ahead of the stopping shock. It is notable that lower initial plenum pressure can generate a faster starting shock M_{98}, inducing faster gas motion behind the starting shock M_8, which is relatively insensitive to the initial plenum pressure (Figure 7 left). Lower plenum pressure initially leads to slower motion of the stopping shock M_{12}, which is subsequently accelerated by fast moving gas ahead of the stopping shock M_2 (Figure 7 right). This mechanism underlies the inlet unstart at a higher initial plenum pressure of $p_i = 0.02p_\infty$.

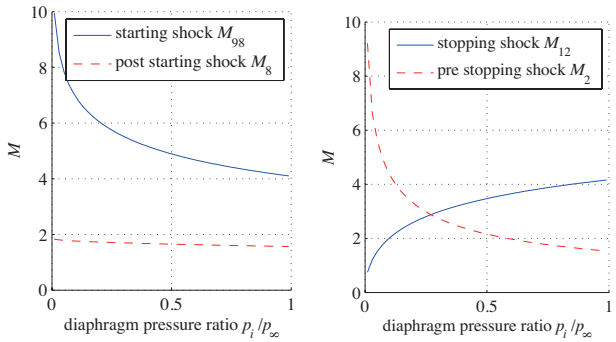

Figure 7. Mach numbers of the starting (left) and stopping (right) shocks in the early phase after diaphragm rupture predicted by the theory.

The flowfields are probed for at $t = 3.2$ and 3.3ms, when the stopping shock lies in the vicinity of the Kantrowitz position. Figure 8 compares the distributions of the stream-thrust-averaged total pressure [6] for these times between $p_i = 0.01p_\infty$ and $0.02p_\infty$, along with the theoretical value for a stopping shock standing at the Kantrowitz position predicted from the normal shock theory and area-Mach number relation. It is found that the total pressure behind the stopping shock is higher than the Kantrowitz value ($p_{02} / p_{01} = 0.057$) for $p_i = 0.01p_\infty$, whereas it is lower for $p_i = 0.02p_\infty$. It can be assumed that the stopping shock heads downstream to allow higher total pressure recovery by a weaker shock in the former case, while it is driven to travel upstream to match the total pressure by a stronger shock in the latter case.

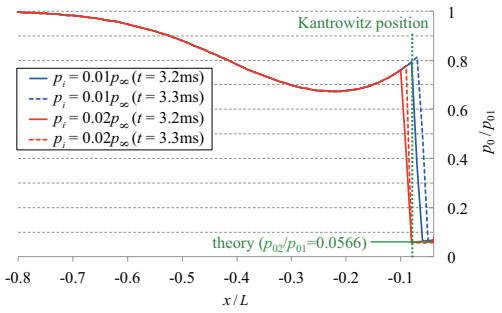

Figure 8. Comparison of total pressure distributions between $p_i = 0.01p_\infty$ and $p_i = 0.02p_\infty$ when the stopping shock stands near the Kantrowitz position $x_k/L = -0.077$ ($t = 3.2$ ms and 3.3 ms).

Viscous Effects

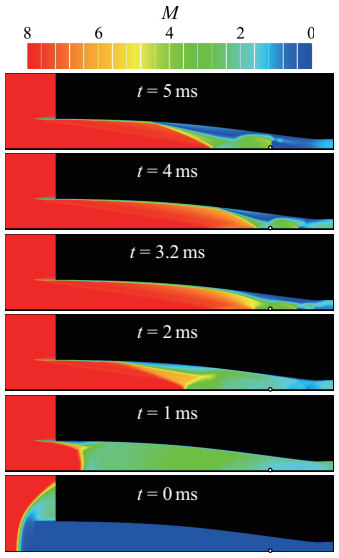

Figure 9. Mach number distribution for a viscous flowfield after diaphragm rupture calculated by CFD for an initial plenum pressure of $p_i = 0.01p_\infty$ (leading to unstarted inlet).

A viscous computation has been performed for diaphragm rupture with an initial plenum pressure of $p_i = 0.01p_\infty$. The snapshots of the transient flowfield are displayed in Figure 9. Both the starting and stopping shocks travel downstream faster than in the inviscid case ($t = 0$ - 2 ms), in the converging duct which has been effectively narrowed by the boundary layer displacement. However, the impingement of a conical shock wave on the inlet surface causes the boundary layer to separate due to adverse pressure gradient ($t = 3.2$ ms). The separated region consequently imposes a higher contraction on the flow, restricting mass flow travelling downstream ($t = 4$ ms). A similar situation occurred in a preceding study [5] where a three-ramp inlet with a comparable contraction ratio started by removing low momentum fluid by boundary layer bleed. A normal shock arises at the centreline, choking the incoming flow, which finally results in an unstarted inlet at about $t = 10$ ms (not presented).

Effects of Diaphragm Mass

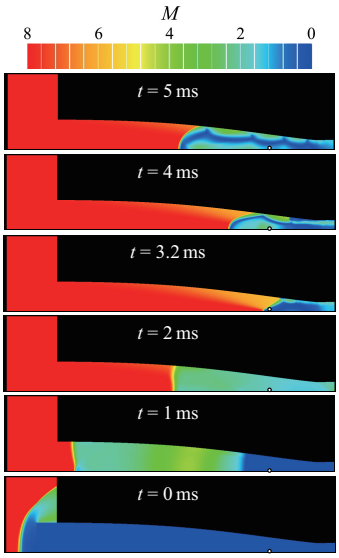

Figure 10. Mach number distribution for a viscous flowfield after rupturing a diaphragm with an area density of 0.0055 kg/m^2 ($\rho_d = \rho_{air} \times 10$) calculated by CFD for an initial plenum pressure of $p_i = 0.01 p_\infty$ (leading to unstarted inlet).

A parametric study was performed to find the effect of diaphragm mass on the starting process. Diaphragm mass was simulated by a 5 mm layer of gas with the same characteristics as air but greater density. For instance a 5 mm thick diaphragm with $\rho_d = \rho_{air} \times 10$ has an area density of 0.0055 kg/m^2. This corresponds to a 4.0 μm thick layer of mylar, a 2.1 μm thick layer of aluminium, and a 0.7 μm thick layer of sheet steel. Figure 10 shows the transient flowfield after rupturing a diaphragm whose area density is 0.0055 kg/m^2 ($\rho_d = \rho_{air} \times 10$). It can be noticed that the shock motion is considerably delayed for both the starting and stopping shock ($t = 1$ ms). The stopping shock is deformed into a conical shock wave ($t = 3.2$ ms) and disgorged upstream, causing the inlet to unstart.

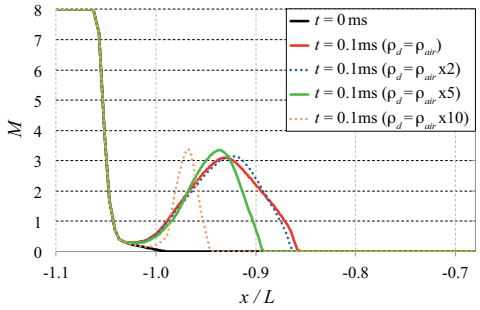

Figure 11. Comparison of centreline Mach number distributions with various diaphragm density at 0.1 ms after diaphragm rupture with an initial plenum pressure $p_i = 0.01 p_\infty$.

Figure 11 shows the centreline Mach number distributions at 0.1 ms after diaphragm rupture for various diaphragm masses. The Mach number rise indicates the flow momentum induced by the passage of the starting shock. The plot demonstrates the impact of the diaphragm mass on the starting shock motion. This results is in agreement with the qualitative tendency of the diaphragm acceleration predicted from Newton's second law: $\rho_d A_i \, dV/dt = (p_{02} - p_i) A_i$, where ρ_d is the area density of the diaphragm, A_i the diaphragm area, p_{02} the stagnation pressure acting on the upstream side of the diaphragm and p_i the plenum pressure on the downstream side. Therefore the initial acceleration of the diaphragm can be prescribed as $dV/dt = (p_{02}/p_\infty - p_i/p_\infty) p_\infty / \rho_d$, where p_{02}/p_∞ is given by the normal shock theory as a function of the freestream Mach number M_∞ and p_{02}/p_∞ is the initial plenum pressure ratio given as an input.

Conclusions

A numerical and analytical study has been conducted for inlet flowfields caused by instantaneous rupture of normal diaphragms in a full Busemann intake for scramjet engines operating at Mach 8. Time-accurate computations have been performed for transient flowfields induced by unsteady flow phenomena, with particular focus on the motion of the starting and stopping shocks. The transient flowfields obtained from numerical simulations are compared with various theories for inviscid flowfields that predict the trajectory of the starting shock and the influence of the plenum pressure on the initial acceleration of the starting and stopping shocks. A started inlet has been achieved for inviscid flow in a Busemann intake with a contraction ratio of 11.4 when the initial plenum pressure ratio is 0.01 of the freestream value, whereas the inlet failed to start with a plenum pressure 0.02 of freestream. Both viscosity and diaphragm mass have been found to have detrimental effects on inlet starting, the former restricting the massflow entry due to flow separation and the latter delaying the motion of starting and stopping shocks. Effects of viscosity play a dominant role in influencing flow and wave motion during starting of a hypersonic air intake with significant contraction. Inviscid flow based results, either in steady of unsteady flow, are not sufficiently accurate to predict the startability of hypersonic air intakes.

References

[1] Boyce, R. R., Tirtey, S. C., Brown, L., Creagh, M., and Ogawa, H., "SCRAMSPACE : Scramjet-based Access-to-Space Systems", AIAA Paper 2011-2297, Apr 2011.

[2] Courant, R. and Friedrichs, K. O., *Supersonic Flow and Shock Waves*, Interscience Publishers, Inc., New York, 1978.

[3] Glass, I. I., Heuckroth, L. E., and Mölder, S., "One-Dimensional Overtaking of a Shock Wave by a Rarefaction Wave", *American Rocket Society*, Vol. 31, 1961, pp. 1453-1454.

[4] Han, Z. and Yin, X., *Shock Dynamics*, Fluid Mechanics and Its Applications, Vol. 11, Kluwer Academic Publishers, Dordrecht/Boston/London, 1993.

[5] Ogawa, H., Grainger, A. L., and Boyce, R. R., "Inlet Starting of High-Contraction Axisymmetric Scramjets", *Journal of Propulsion and Power*, Vol. 26, No. 6, 2010, pp. 1247-1258.

[6] Riggins, D. W. and McClinton, C. R., "Analysis of Losses in Supersonic Mixing and Reacting Flows", AIAA Paper 91-2266, Jul 1991.

[7] Tahir, R. B., Mölder, S., and Timofeev, E. V., "Unsteady Starting of High Mach Number Air Inlets — A CFD Study," AIAA Paper 2003-5191, Jul 2003.

[8] Timofeev, E. V., Tahir, R. B., and Mölder, S., "On Recent Developments Related to Flow Starting in Hypersonic Air Intakes," AIAA Paper 2008- 2512, Apr 2008.